SUPPLEMENTARY INFORMATION

New series of Mononuclear β-diketonate Cerium(III) Field Induced Single-Molecule Magnets

Ànnia Tubau,[a] Silvia Gómez-Coca*,[a,b] Saskia Speed,[a] Mercè Font-Bardía[b] and Ramon Vicente*[a]

Table of Contents

1. Magnetic properties compilation of previous Ce^{3+} compounds.

TableS1. β-diketonate Ce^{3+} mononuclear compounds													
	H (Oe)	Orbach		QTM	Raman		Direct	Local Mode		ΔE_{calc} (cm^{-1})	Calculated g_{xx}, g_{yy}, g_{zz}	Wavefunction analysis of the ground doublet state	Ref
		U_{eff} (cm^{-1})	τ_0 (s)	τ_{QTM} (s)	C ($s^{-1}K^{-n}$)	n	D ($s^{-1}K^{-1}$)	C_{LOC} (s^{-1})	ω (cm^{-1})				
[Ce(fdh)$_3$(bpy)]	2000	23.14	$1.8*10^{-7}$							339.6	0.18, 0.46, 3.79	0,92|±5/2⟩ +0.014|±3/2⟩ +0.066|±1/2⟩	[1]
					0.40	6.0							
[Ce(ntfa)$_3$(MeOH)$_2$]	200	Around 20-30		0.006[(c)]	24.82	2.98	0.00045[(c)]	$1.23*10^9$	32.2	319	1.06, 1.30, 3.16	|±5/2⟩ with contribution of |±3/2⟩	[2]
[Ce(ntfa)$_3$(5,5'-Me$_2$bipy)]	200	Around 20-30		0.06[(c)]	0.86	8.01	0.0006[(c)]	$2.83*10^5$	9.5	258	0.22, 0.37, 3.32	|±5/2⟩ with contribution of |±3/2⟩	
[Ce(ntfa)$_3$(bipy)$_2$]	200	Around 20-30		0.04[(c)]	131.39	1.28	0.0002[(c)]	$6.20*10^5$	15.7	325	0.09, 0.44, 3.91	|±5/2⟩ with contribution of |±3/2⟩	

fdh: 1,1,1-fluoro-5,5-dimethyl-hexa-2,4-dione
ntfa:4,4,4-trifluoro-1-(naphthalen-2-yl)butane-1,3-dionato
[(c)]To be able to compare, τ_{QTM} and D have been calculated applying the corresponding equation to the values obtained from the fit of the dependence with field (B_1 and B_2 for the QTM parameter τ_{QTM} and $A*H^4$ for the Direct parameter D and dT^n, e and f for the Raman C constant).

TableS2. **Mononuclear Ce^{3+} compounds**

Compound[a]	H (Oe)	Orbach		QTM	Raman		Direct	ΔE_{calc} (cm^{-1})	Calculated g_{xx}, g_{yy}, g_{zz}	Wavefunction analysis of the ground doublet state	Ref
		U_{eff} (cm^{-1})	τ_0 (s)	τ_{QTM} (s)	C ($s^{-1}K^{-n}$)	n	D ($s^{-1}K^{-1}$)				
$Li(DME)_3[Ce(COT)_2]$	400	20.85	$1.2*10^{-6}$	0.058				503	2.43, 2.43, 1.03	$\|\pm 1/2\rangle$	3,4
$[Ce(NO_3)_3(18\text{-crown-}6)]$	1000	21.82	$1.7*10^{-7}$								5
		21.06	$2.2*10^{-7}$		0.108	5(fixed)					
		17.79	$9*10^{-7}$		1.5×10^{-3}	9(fixed)					
$[Ce(NO_3)_3(1,10\text{-diaza-}18\text{-crown-}6)]$	1000	30.58	$2.3*10^{-8}$								
		31.28	$2.6*10^{-8}$		0.52	5(fixed)					
		15.99	$6*10^{-6}$		22	9(fixed)					
$[Ce(NO_3)_3(HL_3)]$	3000	26.06	$2.76*10^{-8}$	0.076	0.154	7.36		348	0.06, 0.69, 3.82	$0.94\ \|\pm 5/2\rangle$	6
$[Ce(18\text{-crown-}6)(Cl_4Cat)(NO_3)]\cdot MeCN$	1500				1.22	5(fixed)	31.9	443	0.26 0.40 3.84 [b]<0.5(not visible), 0.81, 3.59	$0.99\|\pm 5/2\rangle$ $+0.004\|\pm 3/2\rangle$ $+0.001\|\pm 1/2\rangle$	7
$[Ce(18\text{-crown-}6)(Br_4Cat)(NO_3)]\cdot MeCN$	800				1.87	5(fixed)	45.4	-	-	-	
$[Ce(NO_3)_3L^5_3]$	200	14.94	$2.7*10^{-7}$					220	1.90, 1.67, 0.26	Mixed m_j states	8
					1.44	6.8	99.5				
$[Ce_{0.29}La_{0.71}(NO_3)_3L^5_3]$	30				0.8	7.55	306.5	220	1.98 1.68 0.01	Mixed m_j states	
$[Ce(Cp^{ttt})_2\{(C_6F_5\text{-}k^1\text{-}F)B(C_6F_5)_3\}]$	1000				0.03	5.37		787	0.1 0.1 4.16 [b]4.22(g_z)	$1\|\pm 5/2\rangle$	9
$[Ce(Cp^{ttt})_2Cl]$					0.005	6.48		353	0.10 0.14 4.09 [b]4.19(g_z)	$0.97\|\pm 5/2\rangle$ $+0.3\|\pm 1/2\rangle$	
$[Ce(Fcterpy)(NO_3)_3(H_2O)]$	2000	13.9	$1.8*10^{-11}$		They used Orbach +Raman functions for the fitting. But the parameters for Raman aren't published.						10
$[Ce(L^6)(NO_3)_3(MeOH)]$	2000	11.82	$3.9*10^{-8}$								11
$[CeL^7F](CF_3SO_3)\cdot 2H_2O$	1200	26.2						503	1.24 1.34 3.30	$0,86\|\pm 5/2\rangle$ $+0.12\|\pm 3/2\rangle$	12
					0.049	6.56					
$[Ce(dppbO_2)Cl_3]$	100	38			31	3.4		291	0.08, 0.82, 2.86	$0.53\|\pm 5/2\rangle$ $+0.27\|\pm 3/2\rangle$ $+0.20\|\pm 1/2\rangle$	13
$[Ce(L^8)(NO_3)_3]$	1500	20.16	$2.0*10^{-10}$	$2.69*10^{-4}$							14

[a]Ligand abbreviations:
COT: bis(trimethylsilyl)cyclooctatetraenyl dianion.
18-crown-6: 1,4,7,10,13,16-hexanoxacyclooctadecane.
1,10-diaza-18-crown-6: 1,4,10,13-tetraoxa-7,16-diazacyclo-octadecane
HL: 2-methoxy-6-[(E)-phenyliminomethyl]phenol
L^5: $tBuPO(NH^iPr)_2$:*tert*-butyl-phosphonic-di(isopropyl)amide
Fcterpy: Fcterpy = 4′-ferrocenyl-2,2′:6′,2″-terpyridine
L^6: N,N'-bis(pyridine-2-ylmethylene)cyclohexane-1,2-diamine.
L^7: 1,4,7,10-tetrakis(2-pyridylmethyl)-1,4,7,10-tetraaza-cyclododecane)
[b] Values obtained from EPR spectra recorded in the X-band (9.4 Hz).
$dppbO_2$: 1,2-bis(diphenylphosphino) benzenedioxide
L^8: macrocyclic Schiff base ligand derived from a template reaction of o-phenylene diamine and pyridine-2,6-biscarboxyaldehide.

TableS3. **Dinuclear Ce^{3+} compounds**

Compound[a]	H (Oe)	Orbach		QTM	Raman		Direct	ΔE_{calc} (cm^{-1})	Calculated g_{xx}, g_{yy}, g_{zz}	Wavefunction analysis of the ground doublet state	Ref
		U_{eff} (cm^{-1})	τ_0 (s)	τ_{QTM} (s)	C ($s^{-1}K^{-n}$)	n	D ($s^{-1}K^{-1}$)				
$[Ce_2(RR\text{-}L^4)_2(\mu\text{-}Cl)_6]$	3000	-	-		The τ vs. T magnetic data was best reproduced with Raman+Direct function combination			[g]Ce1:348 Ce2:320	Ce1: 0.53 0.90 3.06 Ce2: 0.27 0.62 3.07 [e]<0.5, 0.71, 3	Ce1:0.65|±5/2⟩ +0.05|±3/2⟩ +0.3|±1/2⟩ Ce2:0.67|±5/2⟩ +0.07|±3/2⟩ +0.26|±1/2	15

[a]Ligand abbreviations:
L^4: N,N'-bis((2,2-diphenyl-(pyridine-2-yl)methylene)-(R,R/S,S)-ethane-1,2-diamine)
[g] Dinuclear compound with two cristallographically different Ce^{3+} atoms.
[e] Values obtained from EPR spectra recorded in the X-band (9.4 Hz).

Table S4. **Heterometalic Ce^{3+} compounds**

	H (Oe)	Orbach		QTM	Raman		Direct	ΔE_{calc} (cm^{-1})	Calculated g_{xx}, g_{yy}, g_{zz}	Wavefunction analysis of the ground doublet state	Ref.
Compound [a]		U_{eff} (cm^{-1})	τ_0 (s)	τ_{QTM} (s)	C ($s^{-1}K^{-n}$)	n	D ($s^{-1}K^{-1}$)				
$[Ce\{ZnI(L^1)\}_2(MeOH)]BPh_4$	0	14.73	$1.6*10^{-7}$	0.00038				179.5	0.33, 0.48, 4.06 [d]g_z=3.27(9)	0.78|±5/2⟩ -0.10|±3/2⟩	16, 4
$[Ce\{Zn(L^2)(AcO)\}_2]BPh_4$	250	25.8	$2.7*10^{-7}$								17
$[Ce(dmso)_8][Ce(\eta_2\text{-}NO_3)_2(dmso)_4(\alpha\text{-}Mo_8O_{26})_{0.5}][Mo_6O_{19}]$	200	16.9	$2.56*10^{-7}$								18
		3	$2.09*10^{-5}$								
		6.3	$1.12*10^{-6}$								
$[Ce(NO_3)\{Zn(L^2)(SCN)\}_2]$	1000	24.8	$2.2*10^{-7}$								19
$[CeCd_3(Hquinha)_3(n\text{-}Bu_3PO)_2I_3]$	1500	18.8	$8.2*10^{-7}$	2.58[c]	0.13	6.75	0.0209[c]	303	0.02, 0.10, 2.48	0.96|±3/2⟩	20
$[NiCeL^3(NO_3)_3]$	500	5.90[b]	$7.7*10^{-5}$			6.5-9.1					21
$[ZnCeL^3(H_2O)(NO_3)_3]\cdot H_2O$	500	3.20	$2.5*10^{-5}$			6.5-9.1					
$[Zn_2Ce(HL^9)_4(CH_3COO)](NO_3)_2$	200	8.5	$1.9*10^{-4}$	0.15	0.37	4.82	0.7	363	0.07 0.13 4.09	0.98|±5/2⟩ +0.01|±1/2⟩ +0.0004|±3/2⟩	22

[a]Ligand abbreviations:
L^1: 6,6′-(2,2-dimethylpropane-1,3-diyl)bis(azan-1-yl-1-ylidene)bis(methan-1-yl-1-ylidene) bis(2-meth- oxyphenol).
L^2: 6,6′-(ethane-1,2-diylbis(azanylylidene)) bis(methanylylidene) bis(2-methoxyphenol).
H_2quinha: quinaldichydroxamic acid
L^3: 6,6'-((1-phenylpropane-1,2-diyl) bis(azaneylylidene)) bis(mehanylylidene) bis(2-methoxyphenol)
L^9: (E)-2-(((2-(hydroxymethyl)phenyl)imino)methyl)-6-methoxyphenol
[b] value obtained from the Generalized Debye model fit: $\ln(\chi''_M/\chi'_M) = \ln(1/\tau_0) - U_{eff}/(k_BT)$
[c] To be able to compare, τ_{QTM} and D have been calculated applying the corresponding equation to the values obtained from the fit of the dependence with field (B_1 and B_2 for the QTM parameter τ_{QTM} and $A*H^4$ for the Direct parameter D).
[d] value obtained from the HF-EPR spectra.

Table S5. Ce^{3+} Frameworks											
Compound [(a)]	**H (Oe)**	**Orbach**		**QTM**	**Raman**		**Direct**	**ΔE_{calc} (cm^{-1})**	**Calculated g_{xx}, g_{yy}, g_{zz}**	**Wavefunction analysis of the ground doublet state**	**Ref**
		U_{eff} (cm^{-1})	**τ_0 (s)**	**τ_{QTM} (s)**	**C ($s^{-1}K^{-n}$)**	**n**	**D ($s^{-1}K^{-1}$)**				
$\{[Ce_2(2,5\text{-pzdc})_3(H_2O)_4]\}\cdot H_2O$	**2000**	**12.0**	**$99.8*10^{-8}$**		**3285**	**9 (fixed)**	**$18.6*10^{-3}$**	**303**	**3.59, 2.91, 2.03** [(b)]	**$\|\pm 1/2\rangle$** [(b)]	**23a**
	1000	**10.5**	**$65.3*10^{-8}$**		**3411**	**9 (fixed)**	**$19.2*10^{-3}$**				
$[Ce_2Zn_3(oda)_6(H_2O)_6]\cdot 12H_2O$	**2000**	**13**						**326.6**	**1.37, 1.37, 1.16**	**$0.41\|\pm 5/2\rangle + 0.58\|\pm 1/2\rangle$**	**23b**
	2000				**631**	**2.6**					
	1000				**501**	**2.7**					

[(a)] **Ligand abbreviations:**
pzdc: 2,5-pyrazinedicarboxylate dianion.
oda: oxydiacetate
[(b)] **Values obtained from Q-band EPR spectra.**

2. Structural characterization

Table S6. Crystallographic information from the Single Crystal X-Ray Diffraction measurements of compounds **1**, **2** and **3a**

Complex	**$[Ce(Btfa)_3(H_2O)_2]$ (1)**	**$[Ce(Btfa)_3(H_2O)_2]$ (1) r.t.**	**$[Ce(Btfa)_3(phen)]$ (2)**	**$[Ce(Btfa)_3(bipy)(EtOH)]$ (3a)**
Formula	$C_{30}H_{22}CeF_9O_8$	$C_{30}H_{22}CeF_9O_8$	$C_{42}H_{26}CeF_9N_2O_6$	$C_{42}H_{31}CeF_9N_2O_7$
FW [g/mol]	821.59	821.59	965.77	986.81
Crystal System	orthorhombic	orthorhombic	monoclinic	triclinic
Space Group	$P2_12_12_1$	$P2_12_12_1$	$P\ 2_1/c$	P-1
a [Å]	10.8091(3)	10.8548(16)	9.6048(7)	10.8841(8)
b [Å]	14.0772(5)	13.219(2)	36.456(3)	12.3497(9)
c [Å]	21.0790(7)	23.317(4)	10.9642(7)	17.1066(12)
α[º]	90	90	90	88.341(3)
β [º]	90	90	93.010(3)	76.600(3)
γ [º]	90	90	90	66.494(3)
V [Å^3]	3207.42(18)	3345.8(9)	3833.9(5)	2046.0(3)
Z	4	4	4	2
T[K]	100	294	100	100
λ(Mo kα) [Å]	0.71073	0.71073	0.71073	0.71073
D_{calc} [g cm^{-3}]	1.701	1.631	1.673	1.602
μ(Mo Kα) [mm^{-1}]	1.519	1.457	1.283	1.206
R	0.0307	0.0527	0.0332	0.0491
wR_2	0.0633	0.1523	0.0617	0.1253

2.1 Single Crystal X-Ray Diffraction:

Table S7. Crystallographic information from the Single Crystal X-Ray Diffraction measurements of compounds **3-5**

Complex	**[Ce(Btfa)$_3$(bipy)] (3)**	**[Ce(Btfa)$_3$(terpy)] (4)**	**[Ce(Btfa)$_3$(batophen)(DMSO)] (5)**
Formula	$C_{40}H_{26}CeF_9N_2O_6$	$C_{45}H_{29}CeF_9N_3O_6$	$C_{57}H_{41}CeF_9N_3O_7$
FW [g/mol]	941.75	1018.83	1191.05
Crystal System	Monoclinic	Tetragonal	monoclinic
Space Group	$P2_{1/n}$	$P4_3$	$P2_1/c$
a [Å]	11.1505(8)	10.5626(6)	15.4985(6)
b [Å]	22.8068(15)	10.5626(6)	17.0389(7)
c [Å]	15.0009(12)	38.185(2)	20.7744(9)
α[°]	90	90	90
β [°]	99.925(3)	90	107.757(2)
γ [°]	90	90	66.494(3)
V [Å^3]	3757.8(5)	4260.3(5)	90
Z	4	4	4
T[K]	100	100	100
λ(Mo kα) [Å]	0.71073	0.71073	0.71073
D_{calc} [g cm^{-3}]	1.701	1.673	1.602
μ(Mo Kα) [mm^{-1}]	1.519	1.283	1.206
R	0.0307	0.0332	0.0491
wR_2	0.0633	0.0617	0.1253

2.2 Thermo-gravimetric Analysis (TGA):

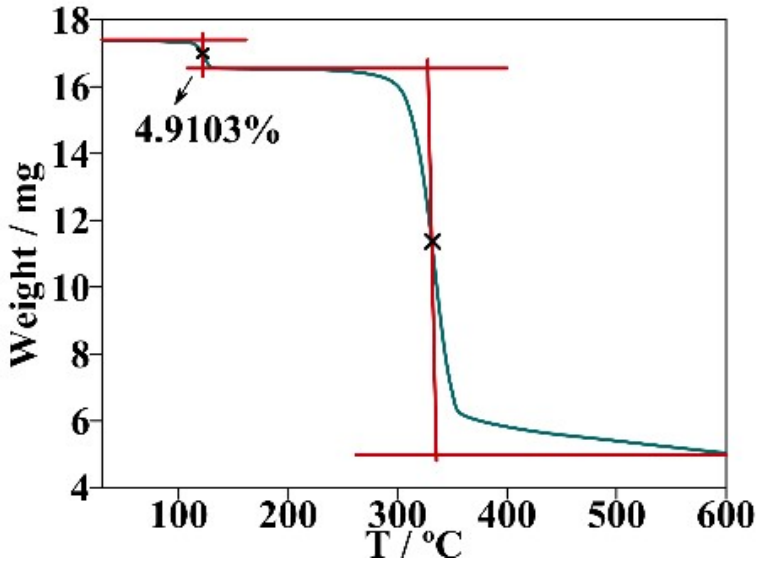

Figure S1. Thermal gravimetric analysis (TGA) on a freshly prepared sample in which probably predominates compound **3a.**

2.3 Powder X-Ray Diffraction:

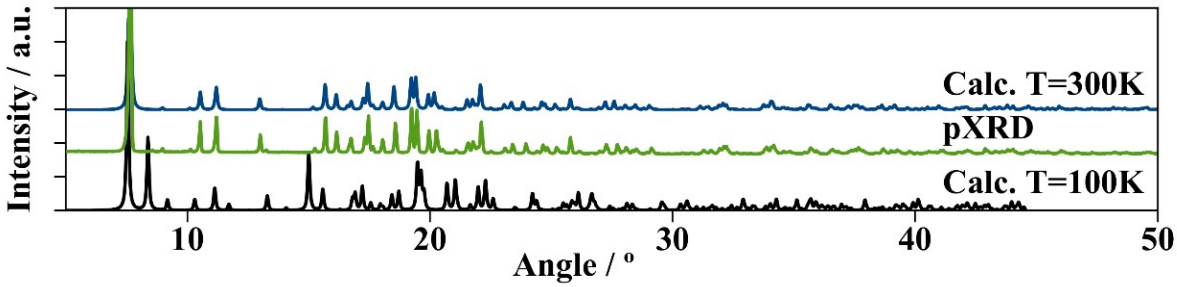

Figure S2. Powder XRD spectra of compound **1** (green), calculated spectra from the crystal structure measured at 100K (black) and at 300K (blue).

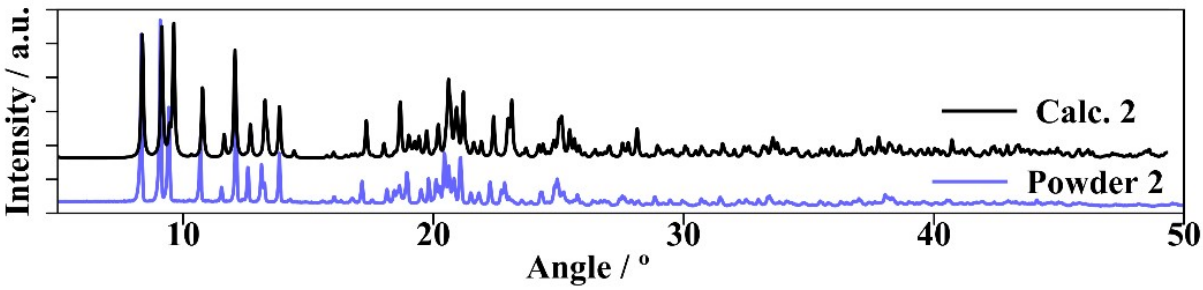

Figure S3. Calculated spectra from the crystal structure (black) compared with the powder XRD spectra of compound **2** (purple).

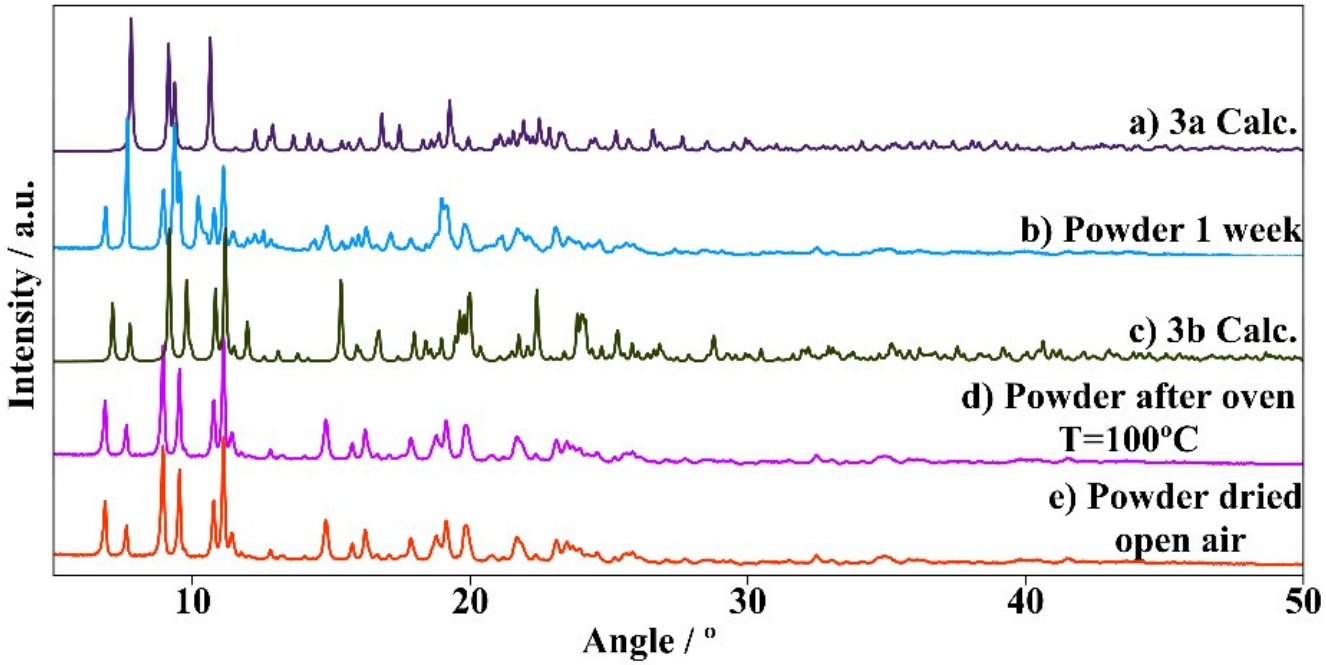

Figure S4. Powder X Ray Diffraction of compounds **3a** and **3**.

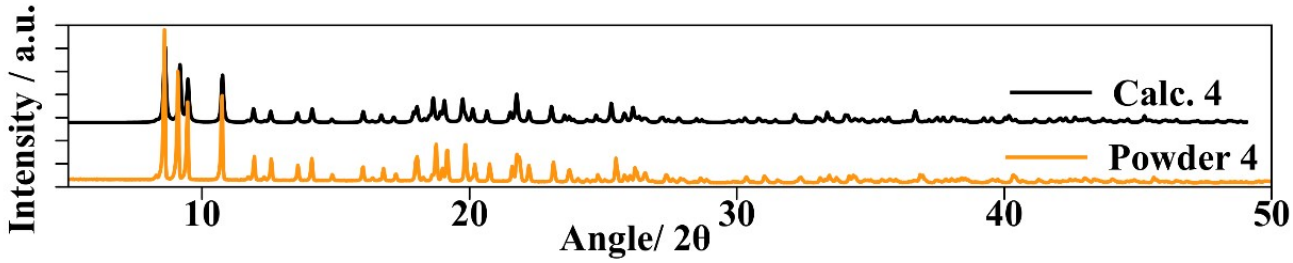

Figure S5. Calculated spectra from the crystal structure (black) compared with the powder XRD spectra of compound **4** (yellow).

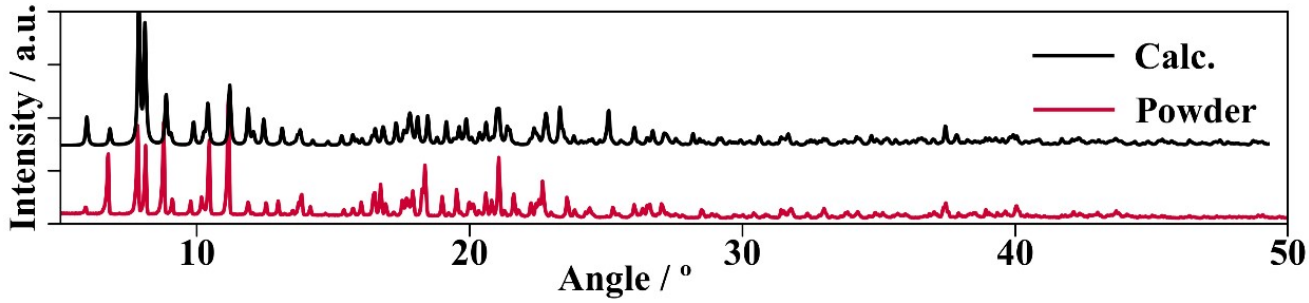

Figure S6. Calculated spectra from the crystal structure (black) compared with the powder XRD spectra of compound **5** (maroon).

2.4 Intermolecular Interactions:

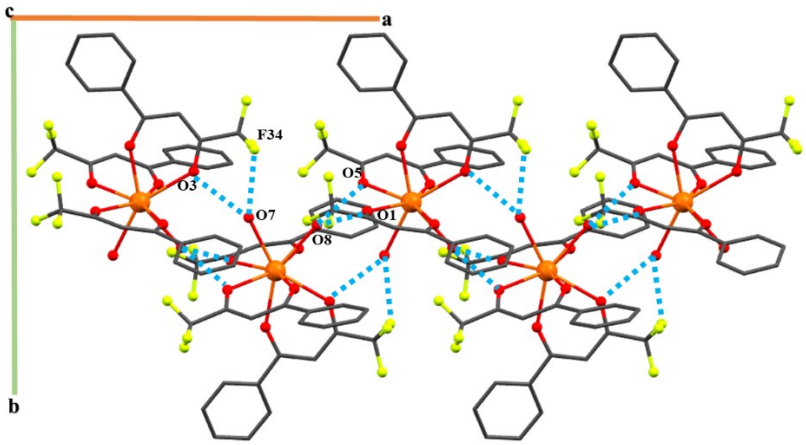

Figure S7. Intermolecular interactions of compound **1**. The H-bond interactions are represented by the blue dotted lines.

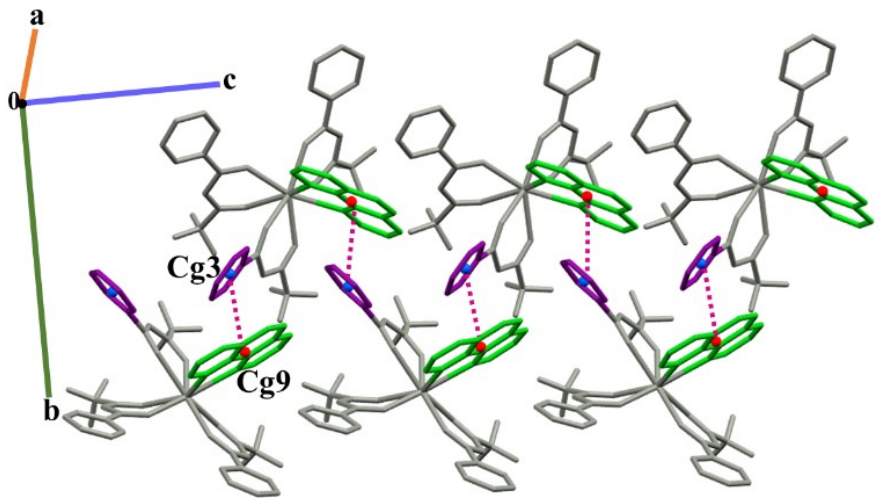

Figure S8. Intermolecular interactions of compound **2**. The π-π stacking interactions are represented by the pink dotted lines.

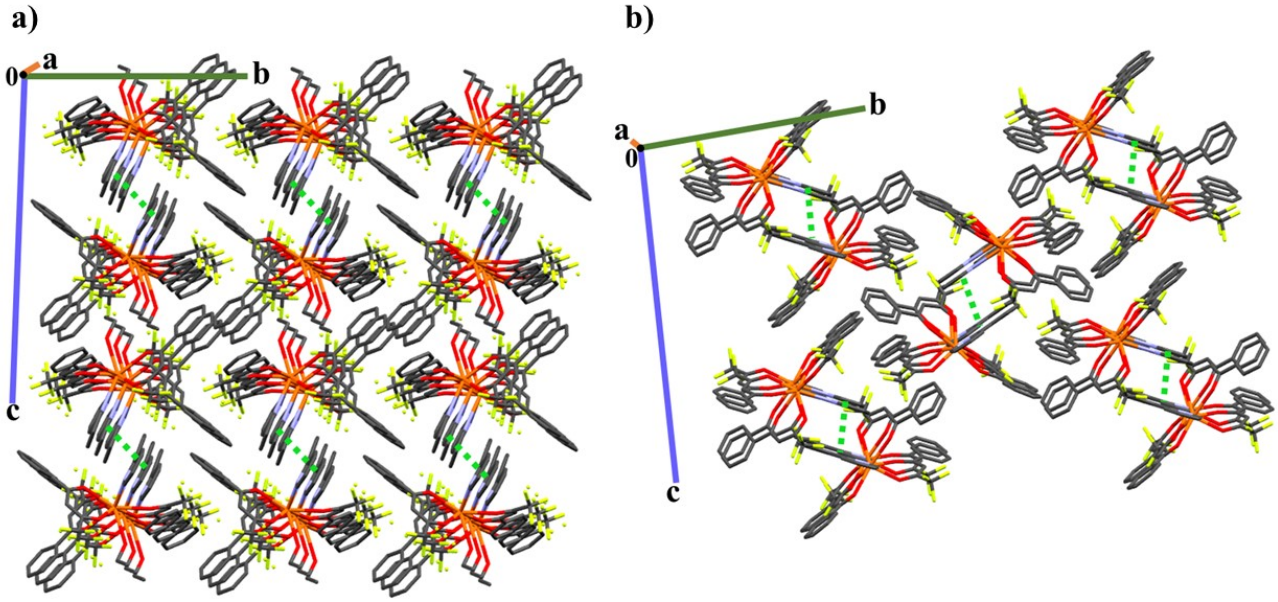

Figure S9. Intermolecular interactions of compound **3**. The π-π stacking interactions are represented by the green dotted lines.

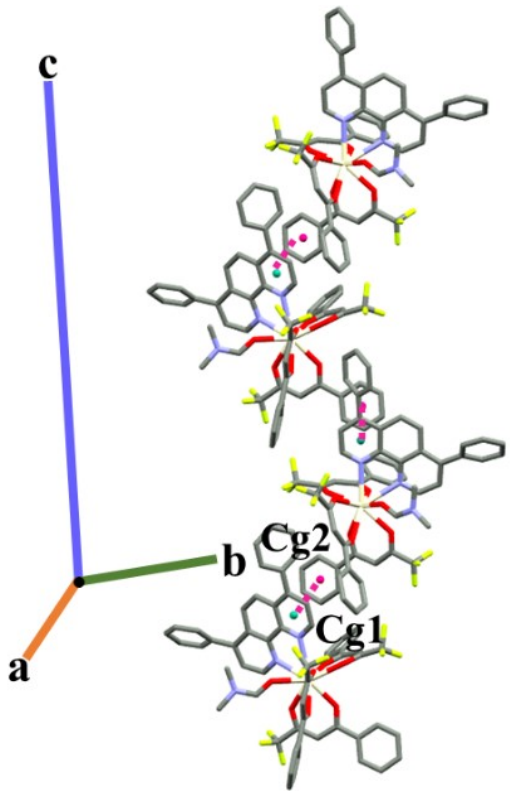

Figure S10. Intermolecular interactions representation of compound **5**. The π-π stacking interactions are represented by the pink dotted lines

3. Magnetic studies and Computational studies:

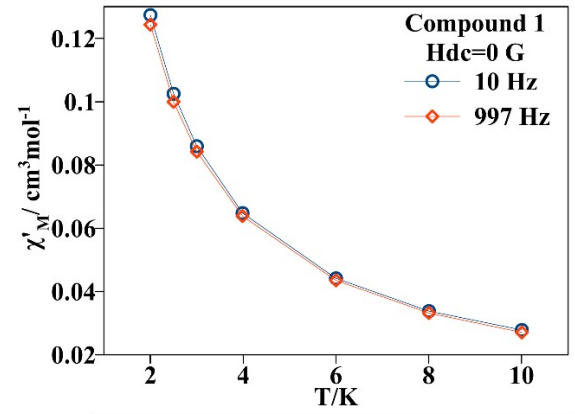

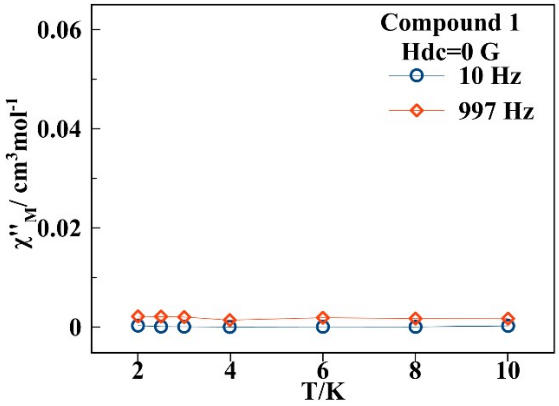

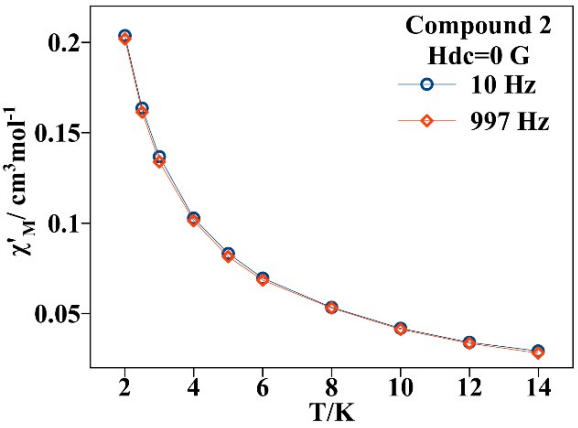

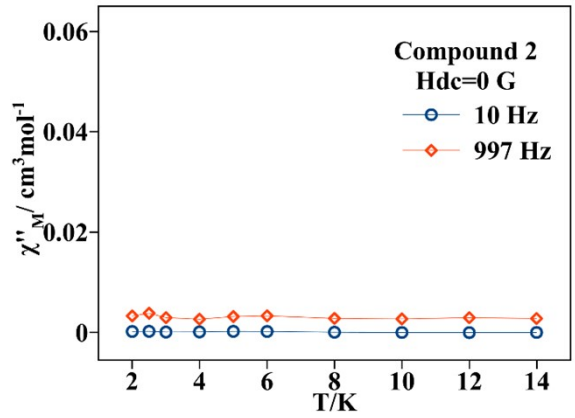

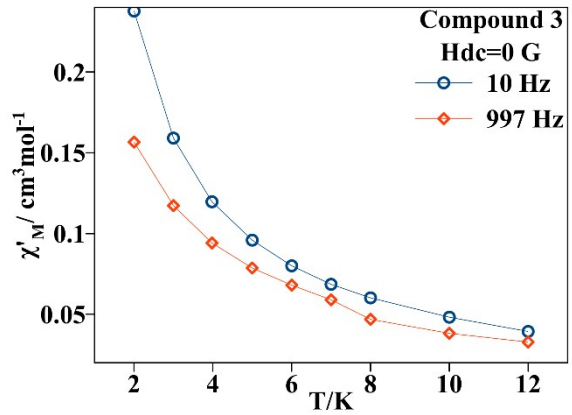

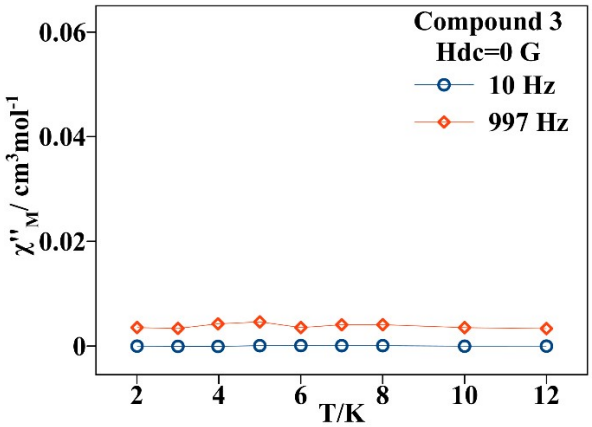

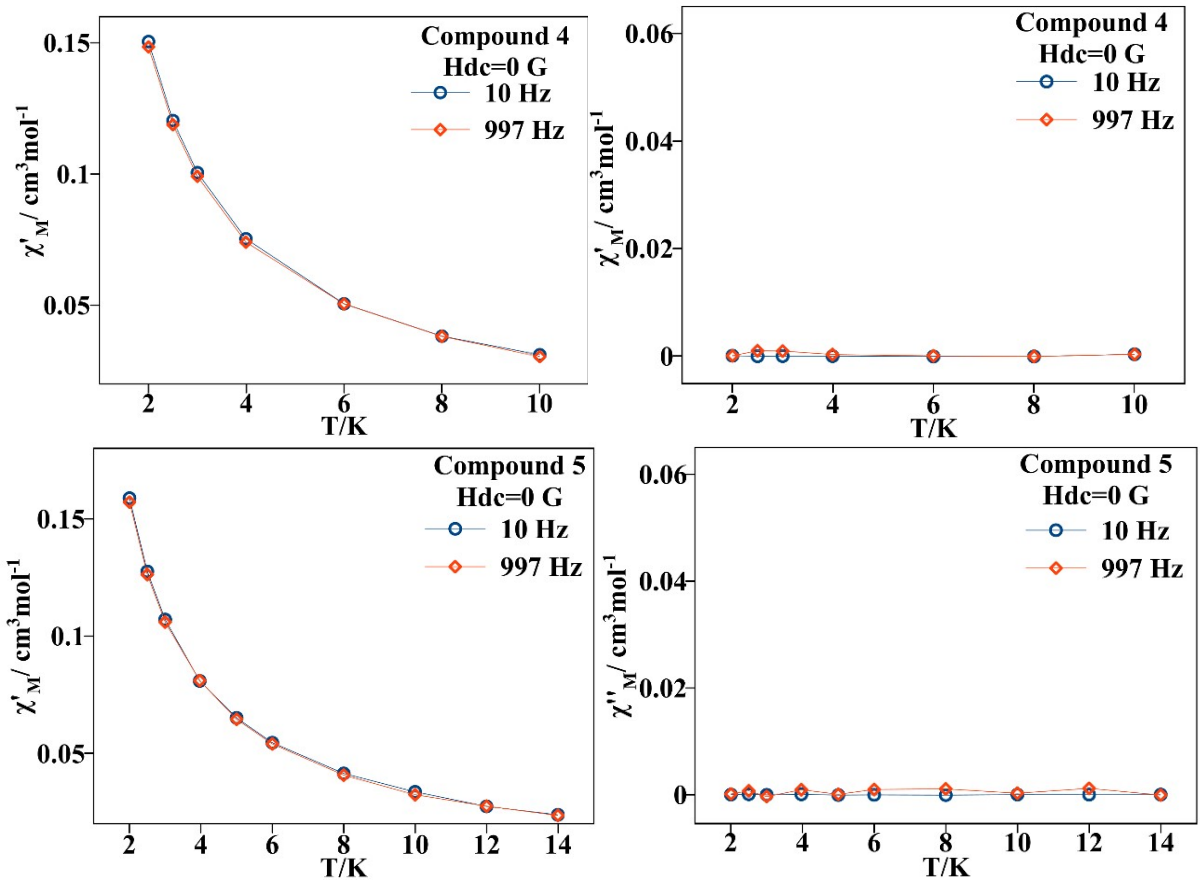

Figure S11. Dynamic magnetic measurements for compounds **1-5** under no external magnetic field (H_{dc}=0G). The measurements were performed in an altern current magnetic field of 4 G oscillating at 10 and 997 Hz. The in-phase (left column) and out-of-phase (right column) magnetic susceptibility components are presented.

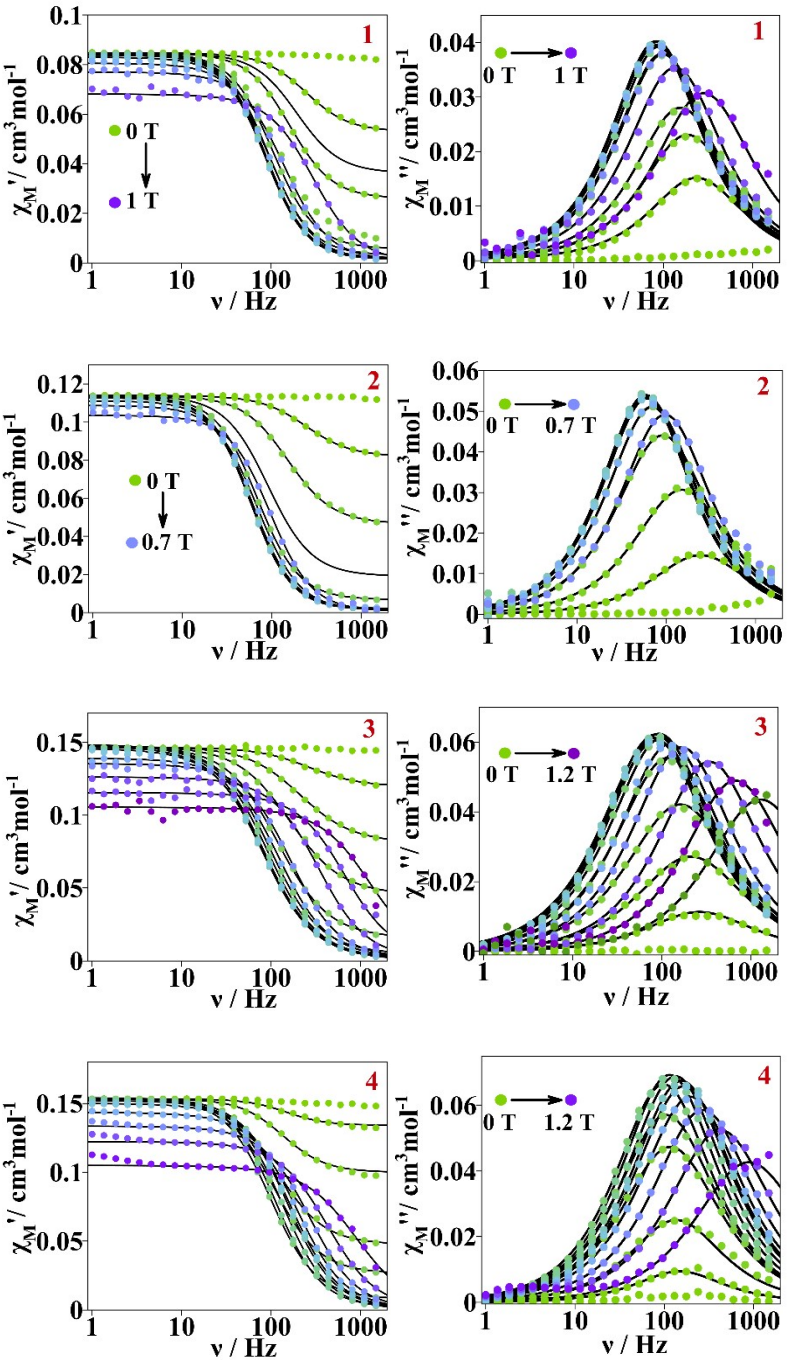
1
0 T
1 T
χM ' / cm3mol-1
χM '' / cm3mol-1
ν / Hz
2
0 T
0.7 T
3
0 T
1.2 T
4
0 T
1.2 T

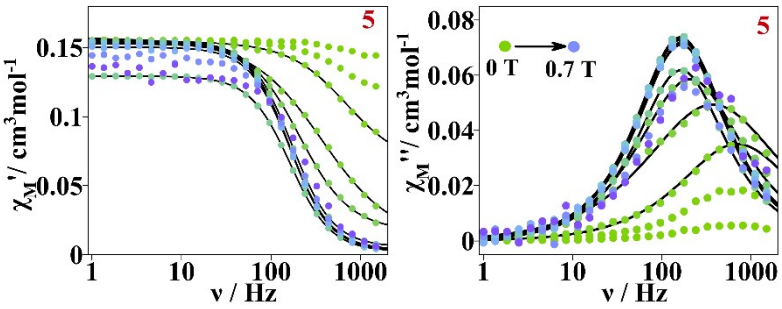

Figure S12. Magnetic susceptibility in-phase (left) and out-of-phase component (right) with frequency plots of compounds **1-5**. The altern current measurements are recorded at different external direct current magnetic fields and at a constant temperature of 2.5 K for **1**, **3** and **5**, of 3.5 K for **2** and 2 K for **4.** Continuous black line refers to the fitting with Eq.S1

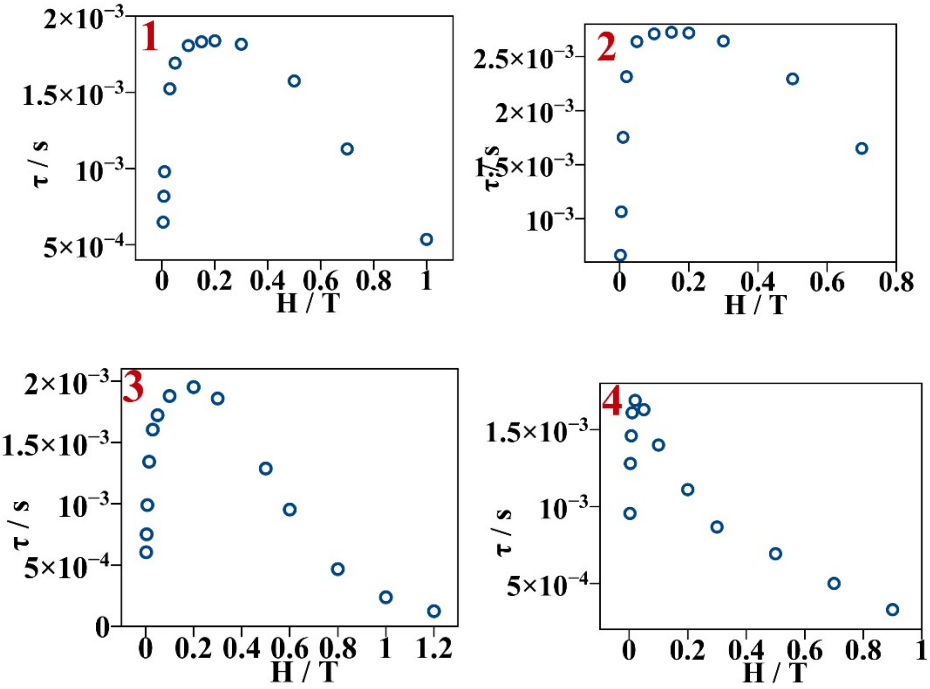

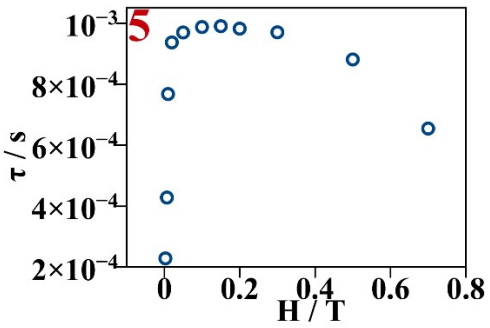

Figure S13. Relaxation of the magnetization times in front of the H_{dc} measured at a constant temperature of 2.5 K for **1**, **3** and **5**, of 3.5 K for **2** and 2 K for **4** at an oscillating frequency of 1-1488 Hz.

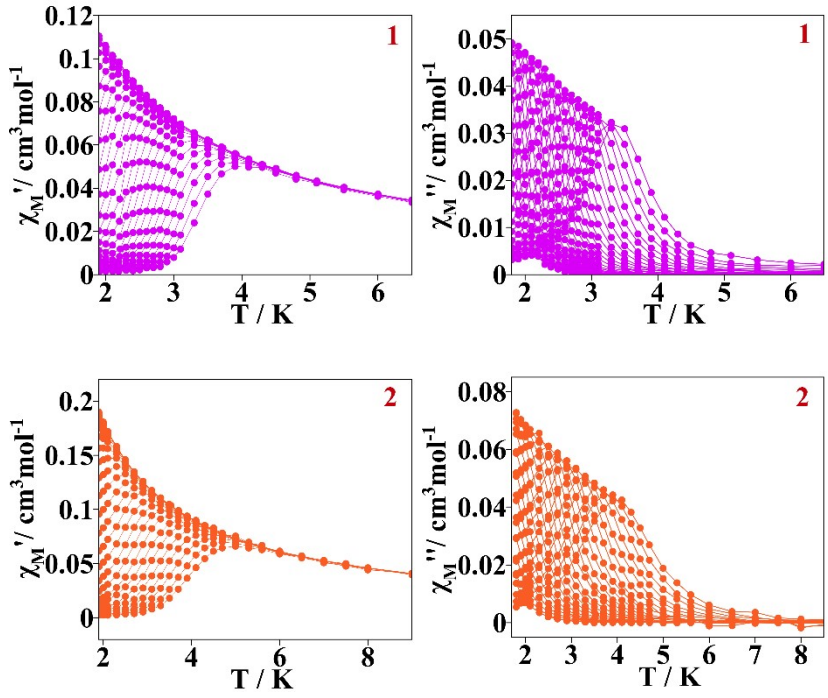

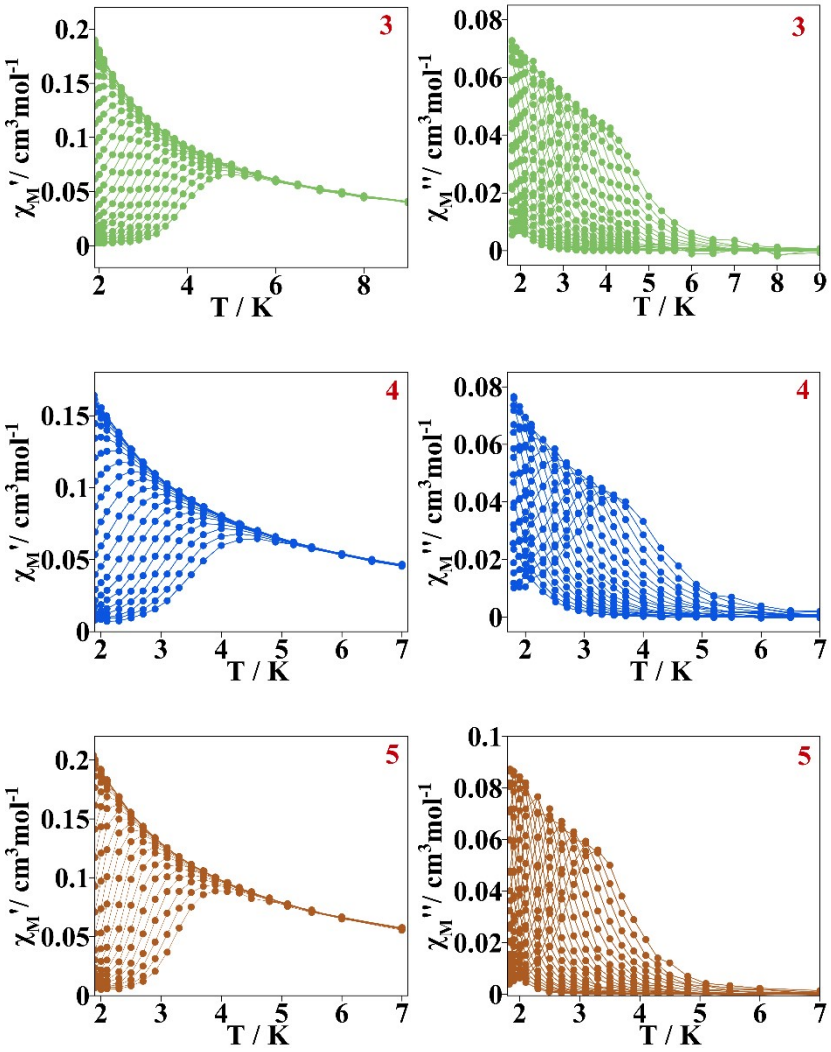

Figure S14. In-phase and out-of-phase magnetic component with temperature plots of compounds **1-5**. The altern current measurements are recorded at different temperatures and at the optimal external magnetic field of 0.1 T for **1-3** and of 0.02 T for **4** and **5**.

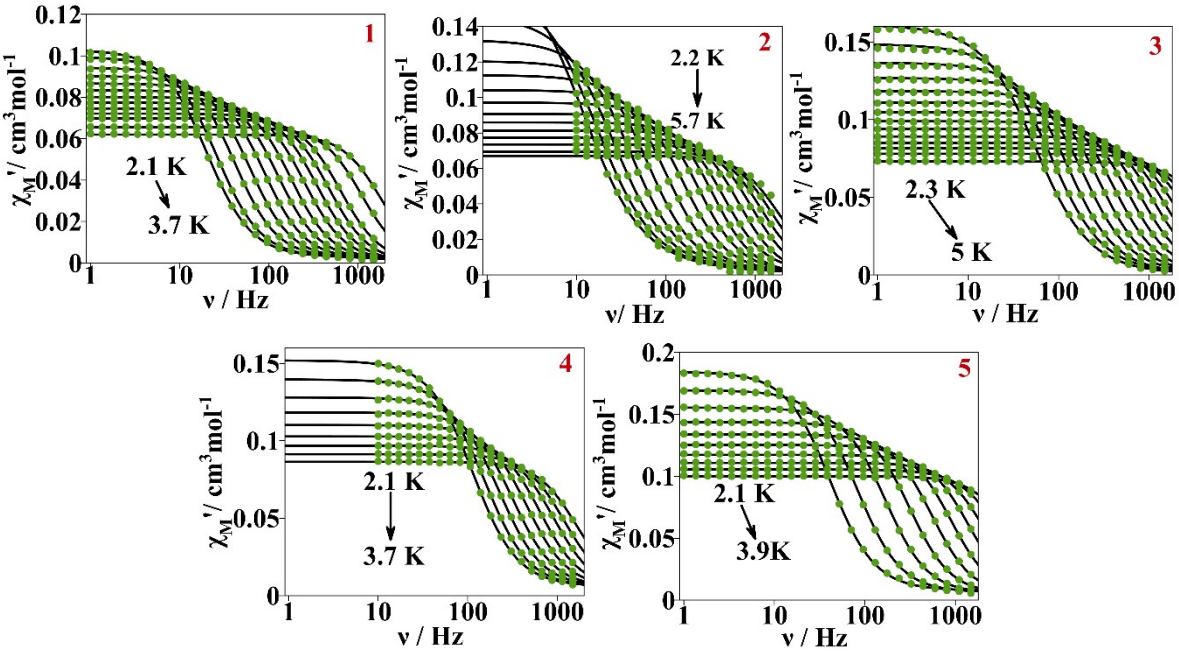

Figure S15. In-phase magnetic susceptibility (χ_M') in front of the oscillating frequency plot measured at a H_{dc} of 0.1 T for **1-3,** and of 0.02 T for **4** and **5.** The continuous lines correspond to the fitting with Equation S1.

$$\chi_{AC}(\omega) = \chi_S + \frac{\chi_T - \chi_S}{1 + (i\omega\tau)^{(1-\alpha)}} \qquad \text{Eq. S1}$$

Equation S1. Generalized Debye model that describes a system with a distribution of the magnetization relaxation time. Where χ_S and χ_T are the adiabatic and isothermal susceptibilities, τ is the relaxation of the magnetization time and ω is the angular frequency of the ac field ($\omega=2\pi f$). χ_T is the susceptibility in the limit of the lowest field frequencies where the thermal equilibrium of the system is observed. χ_S (lower than the χ_T) is observed when the oscillations of the ac field are fast compared to the time constant, τ, and the magnetic system remains isolated from its environment. The α parameter quantifies the width of the τ distribution and it ranges from 0 to 1. The wider the distribution, α acquires a larger value.

Table S8. Values of the parameters obtained from the fit using the Generalized Debye model function for compound **1** from the ac magnetic measurements at different temperatures and constant external magnetic field of 0.1T.				
T/K	$\chi_{S/}$ cm^3mol^{-1}	$\chi_{T/}$ cm^3mol^{-1}	τ /s	α
2	0.00272272	0.10911102	0.01173767	0.00452959
2.2	0.00236562	0.09961818	0.00600891	0.00373991
2.4	0.0019152	0.09020836	0.00261101	0.00324993
2.6	0.00134707	0.08340278	0.00126611	0.0036927
2.8	8.42E-04	0.07738455	6.40E-04	0.00320283
3	5.25E-05	0.07213799	3.39E-04	0.00310032
3.3	1.22E-04	0.06559413	1.46E-04	0.00438026
3.5	1.53E-04	0.06191975	8.84E-05	0.00787016
3.7	0.00152796	0.05890701	5.74E-05	0.02039325

Table S9. Values of the parameters obtained from the fit using the Generalized Debye model function for compound **2** from the ac magnetic measurements at different temperatures and constant external magnetic field of 0.1T.				
T/K	$\chi_{S/}$ cm^3mol^{-1}	$\chi_{T/}$ cm^3mol^{-1}	τ	α
2.2	0.00196871	0.17996929	0.01330594	0.18041189
2.5	0.00144152	0.1633228	0.00930769	0.16429776
2.7	0.00151365	0.14659795	0.00602663	0.13678143
3	0.00205064	0.13251703	0.00384534	0.09992802
3.2	0.00316113	0.12045498	0.0024833	0.06584891
3.5	7.09E-04	0.11263182	0.00157362	0.07423972
3.7	0.00109162	0.10418251	0.00102963	0.05781351
4	0.00177514	0.09708104	6.98E-04	0.0352169
4.2	5.03E-04	0.09067951	4.76E-04	0.02180934
4.5	0.00204468	0.08597008	3.60E-04	0.02461911
4.7	4.60E-04	0.08137422	2.47E-04	0.01700906
5	7.33E-05	0.07728966	1.78E-04	0.01905706
5.2	0.00159915	0.07351246	1.39E-04	0.01256398
5.5	0.00234567	0.06936813	1.07E-04	4.27E-04
5.7	0.00367336	0.06710275	8.97E-05	0.00184958

Table S10. Values of the parameters obtained from the fit using the Generalized Debye model function for compound **3** from the ac magnetic measurements at different temperatures and constant external magnetic field of 0.1T.				
T/K	χ_S/ cm^{3}mol^{-1}	χ_T/ cm^{3}mol^{-1}	τ	α
2.3	2.41E-04	0.16152966	0.00280928	0.00431674
2.5	6.96E-04	0.14880628	0.00187804	0.00466782
2.7	7.52E-04	0.13672155	0.00123476	0.00402393
2.9	0.00124778	0.12681078	8.28E-04	0.00418255
3.1	0.00134343	0.11838076	5.61E-04	0.0028606
3.3	0.00134613	0.11103131	3.87E-04	0.00420111
3.5	0.00112182	0.1048558	2.72E-04	0.00482263
3.7	0.00245962	0.09896616	1.98E-04	0.00369427
3.9	0.0036463	0.09392701	1.45E-04	0.00498305
4.1	0.00377309	0.08913048	1.09E-04	0.00428416

Table S11. Values of the parameters obtained from the fit using the Generalized Debye model function for compound **4** from the ac magnetic measurements at different temperatures and constant external magnetic field of 0.02T.				
T/K	χ_S/ cm^{3}mol^{-1}	χ_T/ cm^{3}mol^{-1}	τ	α
2.1	0.00568958	0.15196177	0.00138392	0.05287601
2.3	0.005134	0.13960549	9.98E-04	0.04570004
2.5	0.00539068	0.12799492	6.99E-04	0.03487154
2.7	0.00539471	0.11827156	4.94E-04	0.02585503
2.9	0.00519114	0.11013289	3.46E-04	0.02126027
3.1	0.00523667	0.10278761	2.47E-04	0.01160956
3.3	0.00337832	0.09687578	1.74E-04	0.0190605
3.5	0.00494219	0.09132465	1.32E-04	0.00602343
3.7	0.00515428	0.08637853	9.78E-05	0.00314095

Table S12. Values of the parameters obtained from the fit using the Generalized Debye model function for compound **5** from the ac magnetic measurements at different temperatures and constant external magnetic field of 0.02T.				
T/K	$\chi_{S/}$ cm^3mol^{-1}	$\chi_{T/}$ cm^3mol^{-1}	τ	α
2.1	0.00741904	0.18448395	0.04998922	0.00381847
2.3	0.00616034	0.16943811	0.03557993	0.00188785
2.5	0.00523933	0.15538703	0.02834122	9.36E-04
2.7	0.00480785	0.14359	0.01709453	5.07E-04
2.9	0.00344719	0.13378131	0.01783388	2.90E-04
3.1	0.0030625	0.12521146	0.01156621	1.77E-04
3.3	0.00440472	0.11720929	0.00112071	1.14E-04
3.5	0.00432505	0.11074461	0.00516482	7.58E-05
3.7	0.00480377	0.10545921	0.02430381	5.08E-05
3.9	0.00805971	0.10001755	0.0117625	3.79E-05

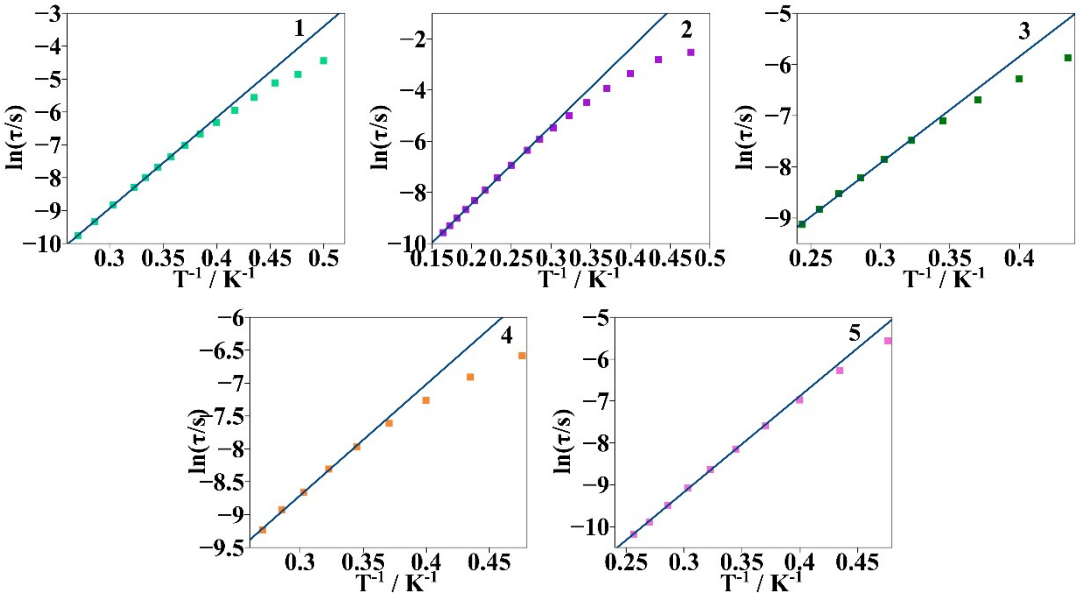

Figure S16. ln(τ) vs. 1/T plot of compounds **1-5**. Continuous blue line corresponds to the fit using the Arrhenius law that describes the Orbach relaxation of the magnetization process:

$$\ln(\tau) = ln(\tau_0) exp\left(\frac{-\Delta E}{k_B T}\right)$$

Table S13. Values obtained from the fitting of ln(τ) vs. 1/T curves using the Arrhenius law that describe the Orbach mechanism.

Arrhenius	**1**	**2**	**3**	**4**	**5**
Δ/cm^{-1}	19.8	18.1	16.4	12.2	16.6
τ_0 /s	2.6e-8	9.7e-7	3.2e-7	8.5e-7	8.3e-8

Table S14. Calculated energy (in cm^{-1}) of the three lowest Kramers doublets and their wavefunction analysis.

Compound	**KDs**	**E (cm^{-1})**	**Wavefunction**
1	GS	0	0.28|±5/2⟩ +0.42|±3/2⟩ +0.30|±1/2
	1st ES	151.9	0.23|±5/2⟩ +0.24|±3/2⟩ +0.53|±1/2
	2nd ES	641.7	0.49|±5/2⟩ +0.34|±3/2⟩ +0.17|±1/2
2	GS	0	0.90|±5/2⟩ +0.005|±3/2⟩ +0.09|±1/2⟩
	1st ES	372.6	0.06|±5/2⟩ +0.27|±3/2⟩ +0.67|±1/2⟩
	2nd ES	661.3	0.04|±5/2⟩ +0.72|±3/2⟩ +0.24|±1/2⟩
3	GS	0	0.87|±5/2⟩ +0.04|±3/2⟩ +0.09|±1/2⟩
	1st ES	289.2	0.06|±5/2⟩ +0.42|±3/2⟩ +0.52|±1/2⟩
	2nd ES	558.1	0.07|±5/2⟩ +0.54|±3/2⟩ +0.39|±1/2⟩
4	GS	0	0.89|±5/2⟩ +0.08|±3/2⟩ +0.03|±1/2⟩
	1st ES	313.9	0.08|±5/2⟩ +0.90|±3/2⟩ +0.02|±1/2⟩
	2nd ES	509.02	0.03|±5/2⟩ +0.02|±3/2⟩ +0.95|±1/2⟩
5	GS	0	0.82|±5/2⟩ +0.04|±3/2⟩ +0.14|±1/2⟩
	1st ES	158.0	0.07|±5/2⟩ +0.78|±3/2⟩ +0.15|±1/2⟩
	2nd ES	344.1	0.11|±5/2⟩ +0.18|±3/2⟩ +0.71|±1/2⟩

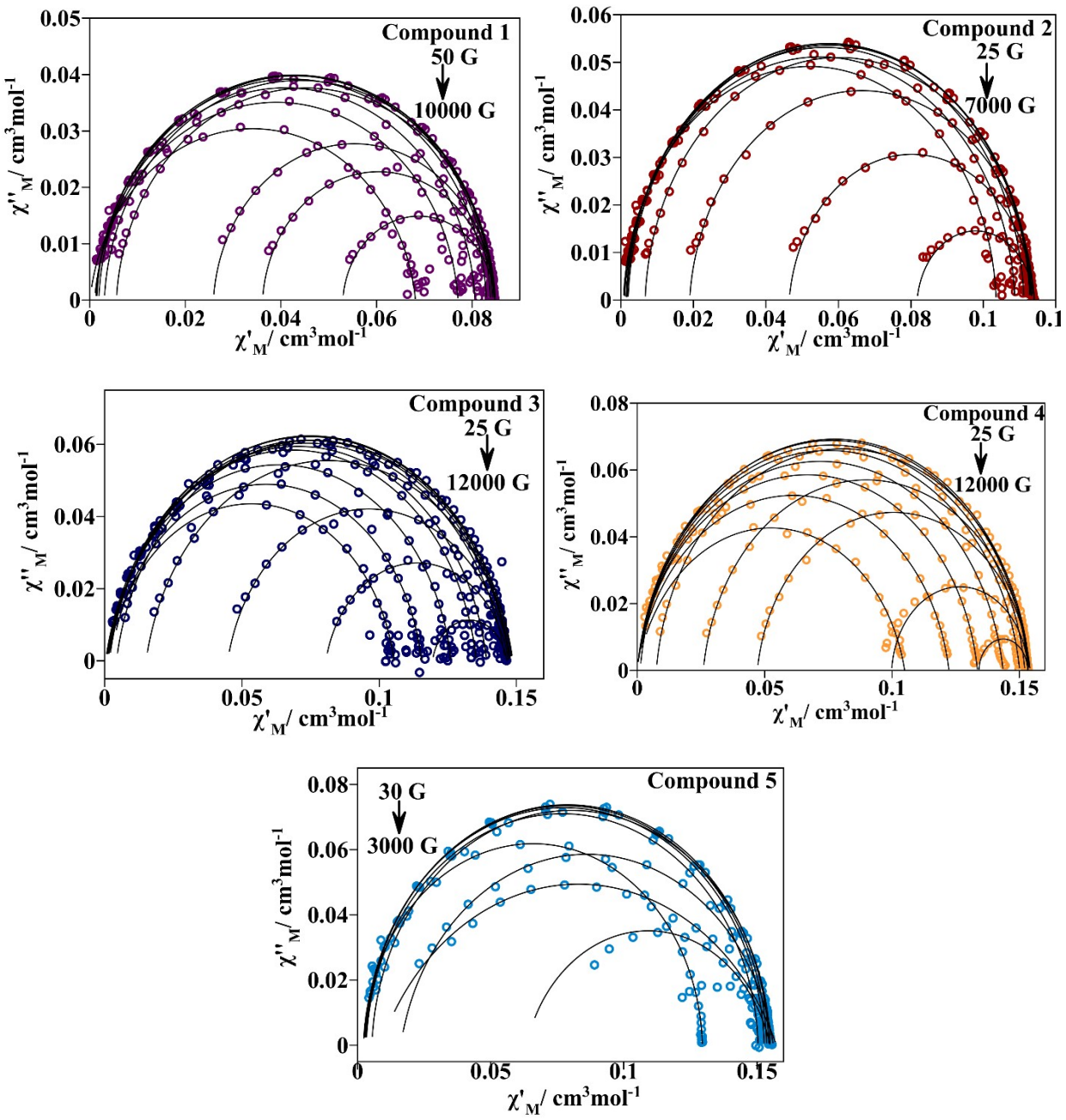

Figure S17. Cole-Cole plots of compounds **1-5** of the altern current magnetic data measured at different direct current external magnetic fields and at a constant temperature.

Table S15. Values of the parameters obtained from the fit using the Generalized Debye model function for compound **1** from the ac magnetic measurements at different direct current external magnetic fields and at a constant temperature of 2.5K.

H/G	τ	**χs**	**χt**	α
50	6.49E-04	0.05295768	0.08476268	0.04208202
75	8.19E-04	0.03615952	0.08471995	0.04104589
100	9.80E-04	0.02589	0.08478455	0.03833559
300	0.00152426	0.00558255	0.08488205	0.03366078
500	0.00169288	0.00305411	0.0847861	0.03032481
1000	0.0018075	0.00188042	0.08455882	0.02441066
1500	0.00183261	0.00145609	0.08426474	0.02329859
2000	0.00183916	0.00137243	0.08384718	0.02264831
3000	0.00181655	0.00130493	0.08299077	0.0260863
5000	0.00157532	0.00130764	0.08058675	0.03305689
7000	0.00112929	0.00102681	0.07707237	0.05128891
10000	5.36E-04	4.01E-05	0.06815536	0.07217991

Table S16. Values of the parameters obtained from the fit using the Generalized Debye model function for compound **2** from the ac magnetic measurements at different direct current external magnetic fields and at a constant temperature of 3.5K.

H/G	τ	**χs**	**χt**	α
25	6.62E-04	0.08174858	0.1140245	0.06576204
50	0.00106407	0.04645884	0.11412017	0.06245169
100	0.00175255	0.01895701	0.11404855	0.04841963
200	0.00231349	0.00669969	0.11343051	0.02849747
500	0.00263717	0.00199307	0.11332312	0.0240103
1000	0.00270909	0.0016741	0.11305778	0.02079883
1500	0.00272395	0.00157938	0.11291049	0.01961294
2000	0.00271782	0.00148477	0.11280279	0.02025025
3000	0.00264233	0.00160211	0.11116022	0.01934466
5000	0.00229259	0.00101339	0.10875354	0.03284961
7000	0.00164951	7.19E-04	0.10354687	0.02879265

Table S17. Values of the parameters obtained from the fit using the Generalized Debye model function for compound **3** from the ac magnetic measurements at different direct current external magnetic fields and at a constant temperature of 2.5K.

H/G	τ	**χs**	**χt**	α
25	6.05E-04	0.11942884	0.14653399	0.11548327
45	7.52E-04	0.08061158	0.14717311	0.12841719
75	9.90E-04	0.04484191	0.14767994	0.12646465
150	0.00134284	0.01511193	0.1478807	0.11322479
300	0.00160451	0.00430077	0.14770493	0.10106212
500	0.00172209	0.00119753	0.14841786	0.10497305
1000	0.00187849	3.58E-04	0.14869074	0.11186906
2000	0.00195112	7.29E-04	0.14755604	0.1154936
3000	0.00185827	8.15E-04	0.14599531	0.11687929
5000	0.00128752	0.00175373	0.13915988	0.09170816
6000	9.53E-04	0.00160174	0.13541034	0.08580357
8000	4.68E-04	0.00112622	0.12618755	0.08883049
10000	2.38E-04	0.00232297	0.11543329	0.09177186
12000	1.25E-04	0.00146233	0.1054581	0.11236558

Table S18. Values of the parameters obtained from the fit using the Generalized Debye model function for compound **4** from the ac magnetic measurements at different direct current external magnetic fields and at a constant temperature of 2K.

H/G	τ	**χs**	**χt**	α
25	0.00107136	0.13410257	0.15319771	0.00864649
40	0.00117117	0.0998473	0.15339134	0.04196866
70	0.00135671	0.04714549	0.15420289	0.07809132
100	0.00150518	0.02593919	0.15406899	0.07361923
200	0.00160705	0.00749712	0.15395939	0.06253502
500	0.00138639	0.00115113	0.15367383	0.06116618
1000	0.00118574	3.84E-05	0.15338681	0.06829937
2000	0.00101998	7.27E-06	0.15212368	0.07603257
3000	9.52E-04	1.10E-05	0.1500817	0.08272699
5000	8.00E-04	3.64E-05	0.14355703	0.08656992
7000	5.84E-04	1.49E-05	0.13352408	0.08290553
9000	3.72E-04	6.48E-05	0.12232399	0.09735895
12000	1.79E-04	4.11E-05	0.10495643	0.1304435

Table S19. Values of the parameters obtained from the fit using the Generalized Debye model function for compound 5 from the ac magnetic measurements at different direct current external magnetic fields and at a constant temperature of 2.5K.

H/G	τ	χs	Xt	α
30	2.29E-04	0.06344523	0.15490883	0.16688048
70	4.28E-04	0.00863449	0.1572994	0.25319771
100	7.68E-04	0.0162768	0.15611982	0.11225024
200	9.37E-04	0.00542627	0.15502828	0.02412203
500	9.70E-04	0.00226558	0.12949495	0.01846429
1000	9.87E-04	0.00310539	0.15442503	0.01623805
1500	9.90E-04	0.00283879	0.15362501	0.01685865
2000	9.82E-04	0.00260818	0.15271509	0.01893931
3000	9.70E-04	0.0032618	0.15043258	0.02276789

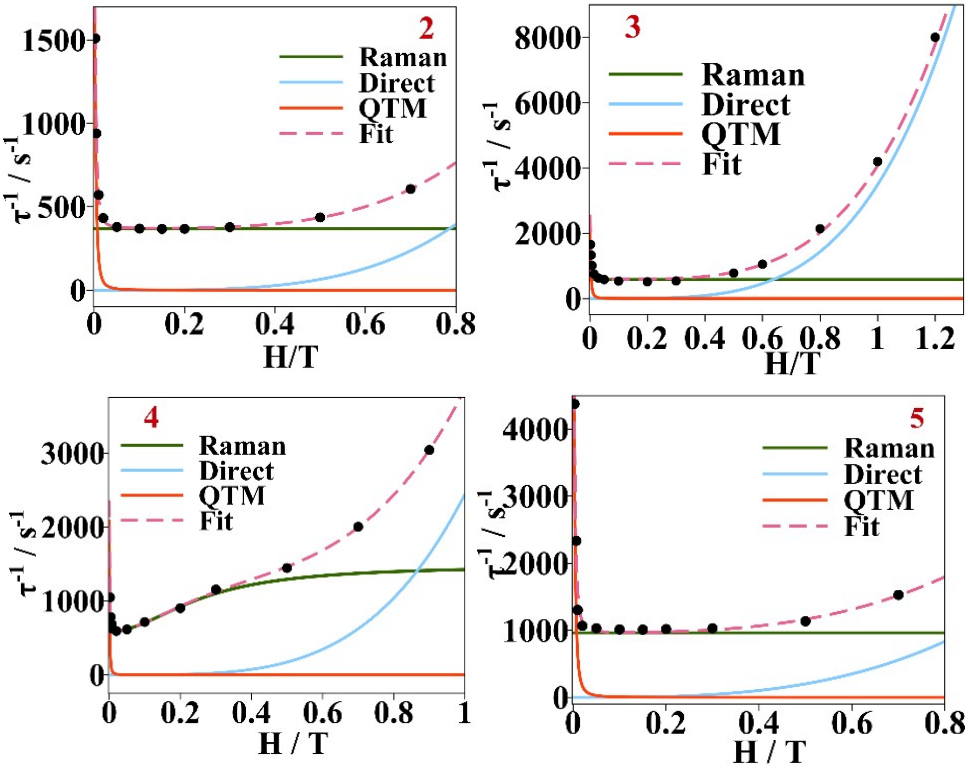

Figure S18. Contribution of Raman, Direct and QTM mechanism to the τ^{-1} vs. H of compounds **2**-**5**. Discontinuous pink line refers to the fit of magnetic data to Eq.3.

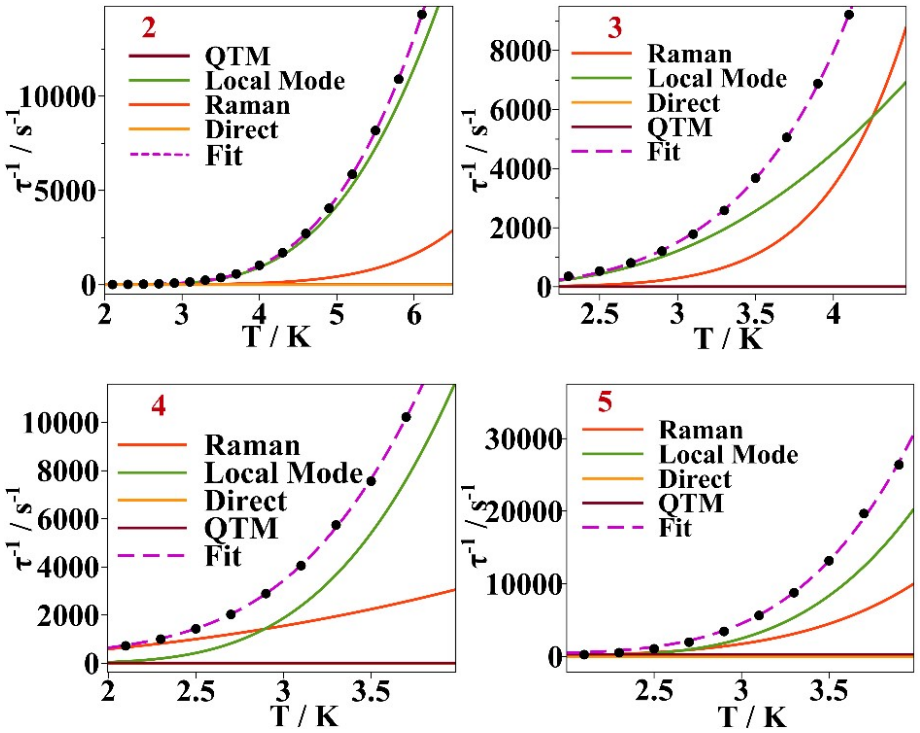

Figure S19. Contribution of Raman, Local Mode, Direct and QTM mechanism to the τ^{-1} vs. H of compounds **2-5**. Discontinuous pink line refers to the fit of magnetic data to Eq.4.

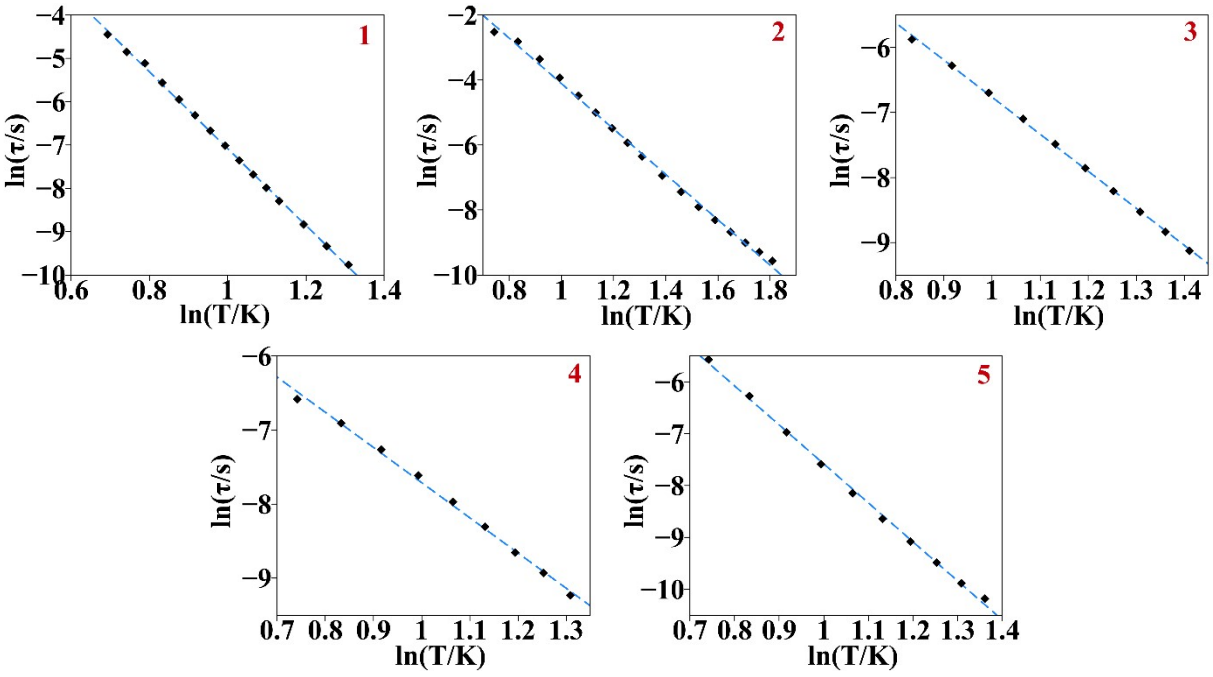

Figure S20. Ln(τ) vs ln(T) plots of compounds **1-5**. Discontinuous blue lines correspond to the fit considering $\ln(\tau) = -n \cdot \ln(T) + \ln(C)$ which describes only the Raman relaxation of the magnetization mechanism.

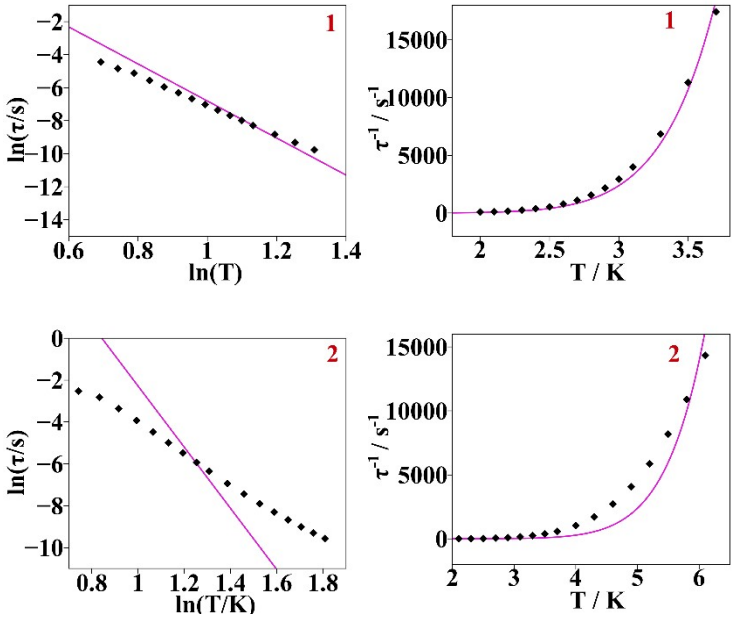

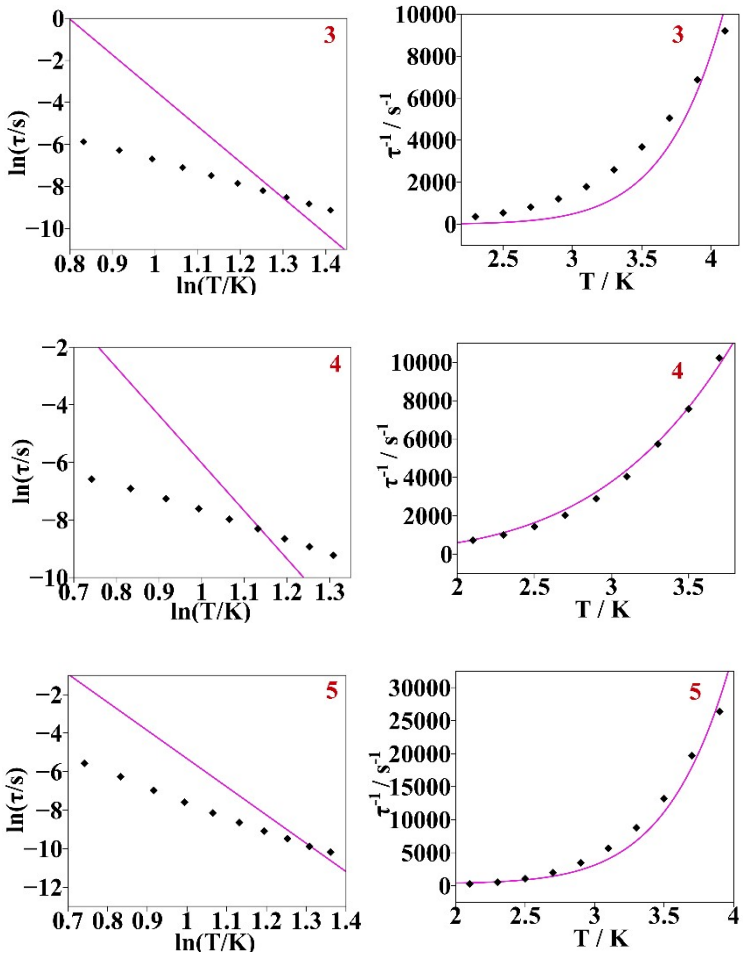

Figure S21. Ln(τ) vs ln(T) plots of compounds **1**-**5**. Continuous pink line refers to the fit with Eq.3 without considering the Local Mode part.

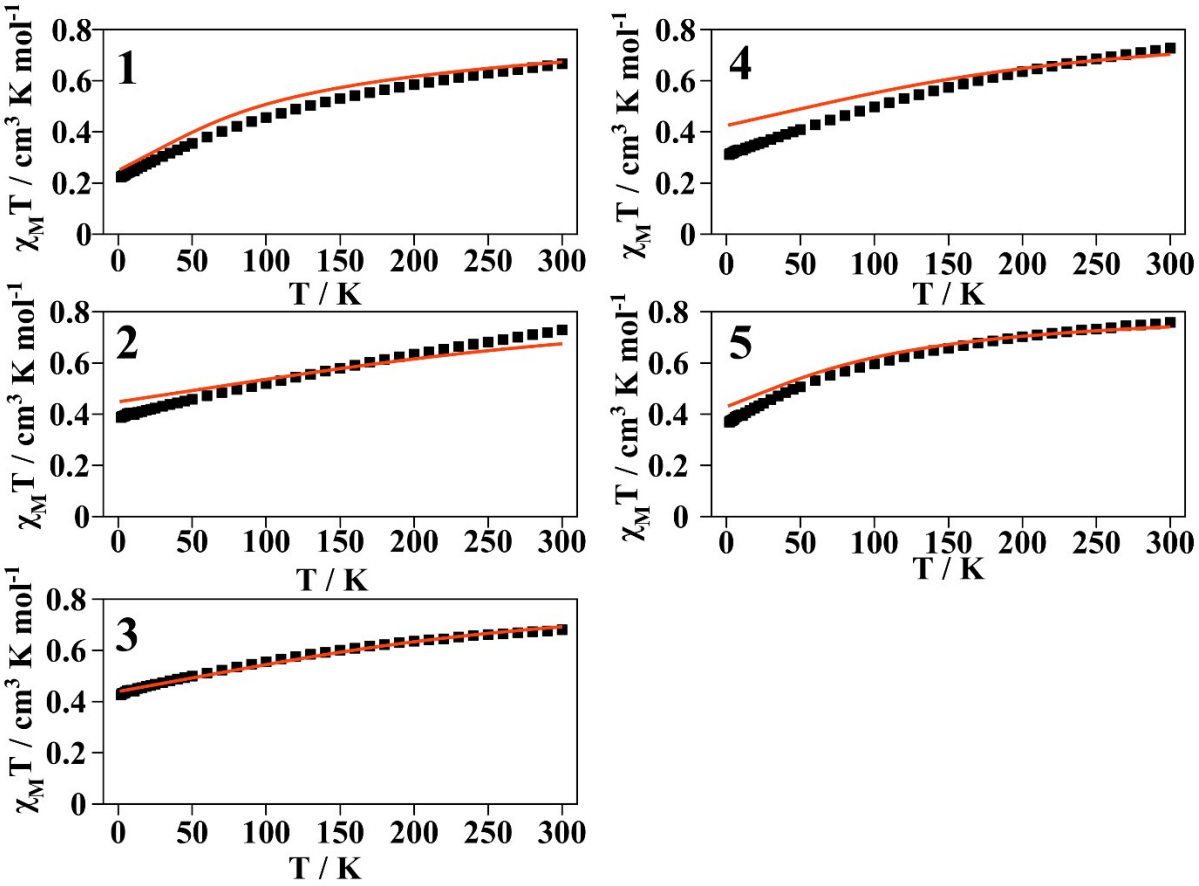

Figure S22. Experimental (symbols) and calculated (lines) of $\chi_M T$ vs T plots of compounds **1** to **5**.

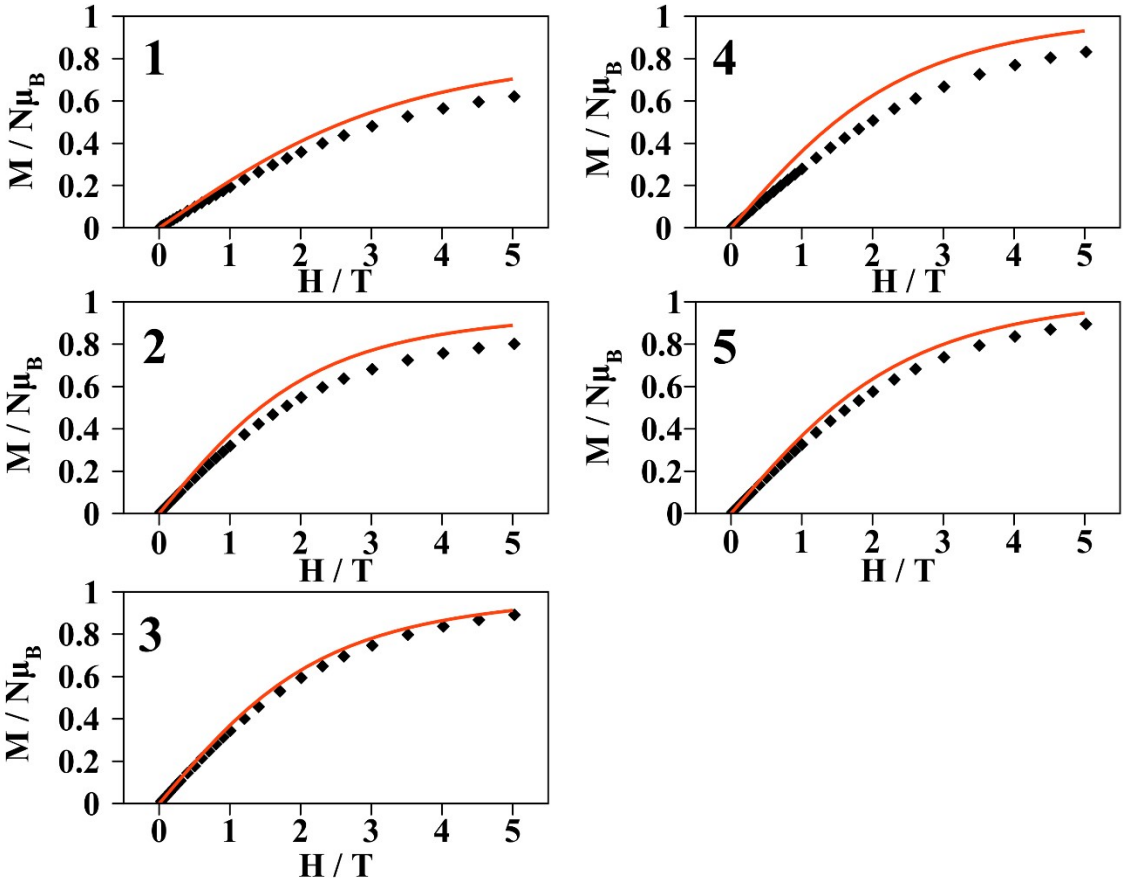

Figure S23. Experimental (symbols) and calculated (lines) of M vs H of compounds **1** to **5**.

Table S20. Energy of the lowest 30 vibrational frequencies calculated with DFT for **1**, **2** and **4**.

Frequency	1	2	4
1	6.9	13.0	5.5
2	10.1	15.0	10.7
3	10.2	16.3	12.7
4	12.3	18.1	14.9
5	14.3	21.3	17.5
6	17.9	24.6	19.6
7	18.7	26.8	21.6
8	21.1	34.7	23.7
9	25.3	35.1	25.4
10	26.7	37.7	27.1
11	41.4	38.9	28.6
12	45.6	40.8	34.5
13	46.2	48.1	36.3
14	52.2	51.9	37.6
15	57.3	71.6	38.7
16	64.2	74.9	41.6
17	68.1	84.6	52.7
18	69.0	89.8	56.7
19	75.1	94.4	61.4
20	78.1	99.9	66.7
21	82.2	107.1	67.1
22	85.8	112.6	74.5
23	93.0	122.4	79.4
24	95.5	127.0	79.6
25	106.3	136.6	82.4
26	110.4	139.9	86.4
27	118.7	153.3	88.7
28	126.0	158.9	100.4
29	139.6	164.2	109.1
30	156.9	173.0	118.4

4. References

1- Magnetic anisotropy investigation on light lanthanide complexes. Dalton Trans., 2018, 47, 1966-1971.

2-Insights into the spin Dynamics of Mononuclear Cerium(III) Singe-Molecule Magnets. Inorg. Chem. 2022, 61, 29, 11124-11136.

3-Structural and magnetic conformation of cerocene [Ce(COT'')2]- exhibiting a uniconfigurational f1 ground state and slow-magnetic relaxation. Dalton Trans., 2014, 43, 2737-2740.

4-Chem. Eur. J. 2015, 21, 13812-13819. Magnetic Relaxation in Single-Electron Single-Ion Cerium(III) Magnets: Insights from Ab Initio Calculations.

5- Light lanthanide Complexes with crown ether and its aza derivative which show slow magnetic relaxation behaviors. Inorg. Chem. 2017, 56, 147-155.

6- Influence of the Ligand on the Slow relaxation of magnetization of unsymmetrical monomeric lanthanide complexes: synthesis and theoretical studies. Inorg. Chem. 2017, 56, 14260-14276.

7- Slow magnetic relaxation in Lanthanoid Crown Ether Complexes: interlay of Raman and Anomalous Phonon Bottleneck Process. Chem. Eur. 2028, 24, 14768-14785

8-A single-ion single-electron cerrous magnets. Dalton Trans., 2019, 48, 15928-15938.

9- Light lanthanide Metallocenium cations exhibiting weak equatorial anion Interactions. Chem. Eur. J. 2019, 25, 7749-7758.

10- A 10-coordinate cerium(III) complex with a ferrocene-based terpyridine ligand exhibiting field-induced slow magnetic relaxation. Polyhedron 188 (2020) 114695.

11-Structural and magnetic studies of mononuclear lanthanide complexes derived from N-rich chiral Schiff bases. Dalton Trans., 2021, 50, 1746.

12-Importance on an Axial LnIII-F Bond across the lanthanide series and Single-Molecule Magnet Behavior in the Ce and Nd analogues. Inorg. Chem. 2022, 61, 9906-9917.

13-Slow magnetic relaxation of mononuclear complexes based on uncommon Kramers lanthanoide ions CeIII, SmIII and YbII. Dalton, Trans., 2022, 51, 12661.

14- A unique and discrete Ce(III) macrocyclic complex exhibits ferroelectric, dielectric and slow relaxation of magnetization properties. M. Wasim, K. Uddin Ansari, P. Kumar, B. Mallick and M. Shanmugam, *Inorg. Chem. Front.,* 2022, 9, 2284.

15- Single-ion anisotropy and Intramolecular interactions in Ce^{3+} and Nd^{3+} dimers. Inorg. Chem., 2021,60,8692-8703.

16- Linear trinuclear Zn(II)-Ce(III)-Zn(II) complex which behaves as a single-molecule magnet. Dalton Trans., 2013, 42, 2683

17- SMM behavior observed in Ce(III)Zn(II)2 linear trinuclear complex. Chem. Lett. 2013, 42, 1276-1278.

18- Single-molecule magnet behavior in polynuclear assembly of trivalent cerium ions with polyoxomolybdates. Dalton Trans., 2015, 44, 16458-16464.

19- Slow magnetic relaxation of light lanthanide-based linear LnZn2 trinuclear complexes. Dalton Trans., 2015, 44, 18276-18283.

20- Unprecedent hexagonal bipyramidal single-ion magnets based on metallacrows. Chem. Commun., 2016, 52, 13365.

21- Enhancement of magnetic relaxation properties with 3d diamagnetic cations in $[Zn^{II}Ln^{III}]$ and $[Ni^{II}Ln^{II}I]$, Ln^{III}=Kramers lanthanides.

22- Zero-field slow magnetic relaxation behavior of Zn2Dy in a family of trinuclear near-linear Zn2Ln complexes: synthesis, experimental and theoretical investigations. Dalton Trans., 2022, 51, 8766.

23- a) Photoluminescent and Slow Magnetic Relaxation Studies on Lanthanide(III)-2,5-pyrazinedicarboxylate Frameworks. Inorg. Chem. 2017, 56, 2108-2123.b) A. López, C. Cruz, V. Paredes-García, V. Veiga, F. Lloret, J. Torres and R. Chiozzone, *New J. Chem*., 2023, **47**, 21781-21789.